



A New Thermophoretic Precipitator for Collection of Nanometer-Sized Aerosol Particles

David Gonzalez,¹ Albert G. Nasibulin,¹ Anatoli M. Baklanov,²
 Sergei D. Shandakov,³ David P. Brown,¹ Paula Queipo,¹ and Esko I. Kauppinen^{1,4,*}

¹Department of Engineering Physics and Mathematics and Centre for New Materials,
 Helsinki University of Technology, Espoo, Finland

²Institute of Chemical Kinetics and Combustion, Siberian Branch of the Russian Academy of Sciences,
 Novosibirsk, Russian Federation

³Kemerovo State University, General Physics Department, Kemerovo, Russian Federation

⁴VTT Processes, Aerosol Technology Group, Espoo, Finland

A new thermophoretic precipitator (TP) has been designed and used for the collection of nanosized aerosol particles. NaCl and Fe particles, with mean diameters of 55 nm and 3.6 nm, respectively, were used to determine the thermophoretic deposition efficiency as well as the uniformity of the deposition. When the average temperature gradients applied were 2200 K/cm and 2400 K/cm, a high thermophoretic deposition efficiency, close to 100%, was attained at aerosol flow rates below 15 sccm. A gradual decay in the efficiency was observed as the flow rate was increased. Theoretical calculations of particle deposition efficiency were in good agreement with experimental data. The deposition along the TP was shown to be homogenous on a millimeter scale for both NaCl and Fe particles collected on thin foil substrates and microscope grids, respectively. Finally, the thermophoretic precipitator was used to efficiently deposit Fe nanoparticles on a substrate for the subsequent growth of carbon nanotubes.

1. INTRODUCTION

Nanotechnology is often described as having “revolutionary” potential in terms of its possible industrial applications. It offers solutions to many current problems by means of better performing materials, components and systems and also contributes to solving global and environmental challenges. Nanomaterials and, in particular, nanoparticles are at the forefront of this nanotechnology wave (Fu et al. 2004; Pitkethly 2003; Pui and Chen

1997). In this sense, it is apparent that there is an urgent need to improve the synthesis, collection and characterization methods of particles in the nanometric size range. This would enable a better understanding of both the intrinsic properties (morphology, structure, chemical composition, etc.) and the mechanisms of the processes in which nanoparticles are involved.

Thermophoresis, described as a physical phenomenon in which aerosol particles, subjected to a temperature gradient, move from high- to low-temperature zones of the gas, has attracted considerable attention for collection of submicrometer and nanometer particles (Zheng 2002; Kodas and Hampden-Smith 1999). In fact, this phenomenon has been extensively studied both theoretically and experimentally (e.g., Brock 1962; Montassier et al. 1991; Stratmann et al. 1994; Brown et al. 1994; Romay et al. 1998; Tsai et al. 2004). Thermophoresis has been exploited in the design of thermophoretic precipitators to deposit particles from gas streams. The first thermophoretic precipitator employed for aerosol sampling was constructed by Green and Watson (1935). The device, comprising an electrically heated nichrome (NiCr) wire positioned midway between two glass microscope cover slips, was, for many years, the reference sampler for measuring dust concentrations in British mines. A number of different thermophoretic precipitators have been developed over the years, many of them focused especially on achieving more uniform particle deposition (Kethley et al. 1952; Wright 1953). These devices are based on plane-to-plane precipitation, which allowed lower operating temperatures since particles were exposed to the thermophoretic force for a longer time. Most recently, coinciding with the emergent interest of the scientific community in nanotechnology, new thermophoretic precipitators were constructed for the collection of nanoparticles characterization and analysis (Tsai and Lu 1995). Maynard (1995) and Bang et al. (2003) developed thermophoretic precipitators for scanning transmission electron microscopy analysis of ultrafine aerosol particles, which allowed the precipitation of

Received 21 April 2005; accepted 30 September 2005.

Address correspondence to Esko I. Kauppinen, VTT Processes, Aerosol Technology Group, PO Box 1602, FIN-02044 VTT, Espoo, Finland. E-mail: esko.kauppinen@vtt.fi

This work was supported by the Academy of Finland and the European Community Research Training Network “Nanocluster” (grant No HPRN-CT-2002-00328). One of the authors (A.M.B.) thanks Russian Foundation for Basic Researches for the financial support (Project No 04 03 33163).

particles onto microscope support grids. Even though uniform particle deposition on the substrate over a few micrometers was attained, these designs led to non-homogeneous deposits on a larger scale.

The present study describes the development and utilization of a new thermophoretic precipitator for the collection of aerosol particles, especially, in the nanometer size range. The utility of this device is determined on the basis of the thermophoretic deposition efficiency as well as the degree of homogeneity of the deposition in the millimeter scale. Statistical measurements of sizes of deposited particles in different zones of the substrate are assessed. Experimental findings are compared with theoretical predictions. An original application of the TP for the synthesis of carbon nanotubes (CNTs) using thermophoretically deposited Fe particles is also described in this work.

2. DESIGN OF THE THERMOPHORETIC PRECIPITATOR

A schematic cross section of the thermophoretic precipitator (TP) is shown in Figure 1. This device employs an electrically heated plate and a water cooled plate with an aerosol sample flow through the gap between them. The temperature of the cold plate is controlled by circulating cold tap water through an adjacent cooling jacket. The temperature gradient (∇T) is varied by changing the voltage applied to the hot element and/or by the separation distance between the two plates, h . In the embodiment tested, the plates are separated by a thermal insulating gasket and the distance between them is kept at 0.55 mm. A notable advantage of depositing particles using the TP is the possibility of employing many different types of substrates. In this work, aerosol particles were thermophoretically deposited on substrates supported on a polished copper plate having pre-

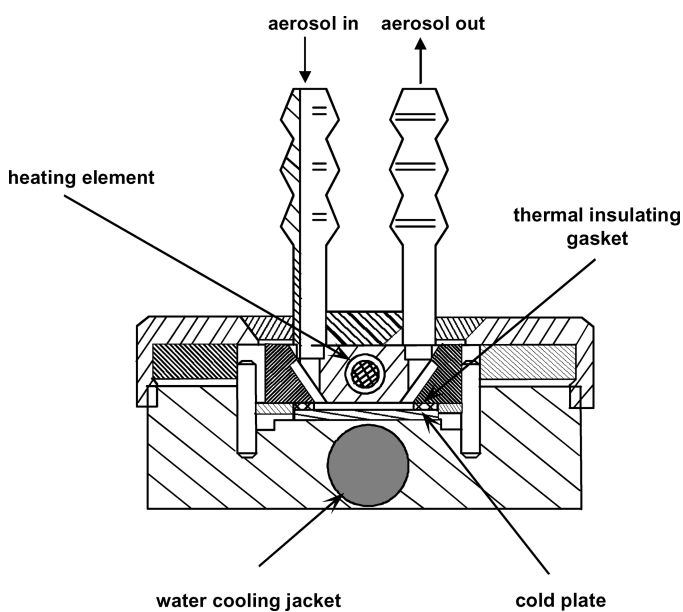


FIG. 1. Schematic cross section of the TP along the centre of the precipitator, following the flow.

cipitation area dimensions with width ($a = 6$ mm and length, $l = 9.3$ mm). This device also allows particle collection on electron microscope support grids by using a stainless steel holder placed on the copper plate. This considerably reduces the complexity of transferring collected particles substrates and facilitates their further utilisation in other processes and/or their analytical characterization.

In order to estimate the temperature and velocity profiles inside the TP, two-dimensional calculations of the flow were carried out using the StreamWise combined CFD/Aerosol code (Brown et al. 2005). Boundary conditions were approximated from available experimental data for Fe particles, as will be discussed later. The flow (27 sccm) of H_2/N_2 (mole component ratio 7/93) through the TP was calculated using constant temperature boundary conditions at the cold wall (279 K) and hot wall (401 K) (giving an average ∇T of 2200 K/cm). The inflow temperature of the TP was assumed to be 298 K. Other exposed surfaces were assumed to be adiabatic. Buoyancy effects were included in the calculation. Results are shown in Figure 2 (27 sccm). The flow was found to be largely non-recirculating in spite of the large turning angles and buoyancy and the temperature gradient in the sampling channel was found to be very uniform. Similar behavior was found for higher flow rates (up to 91 sccm).

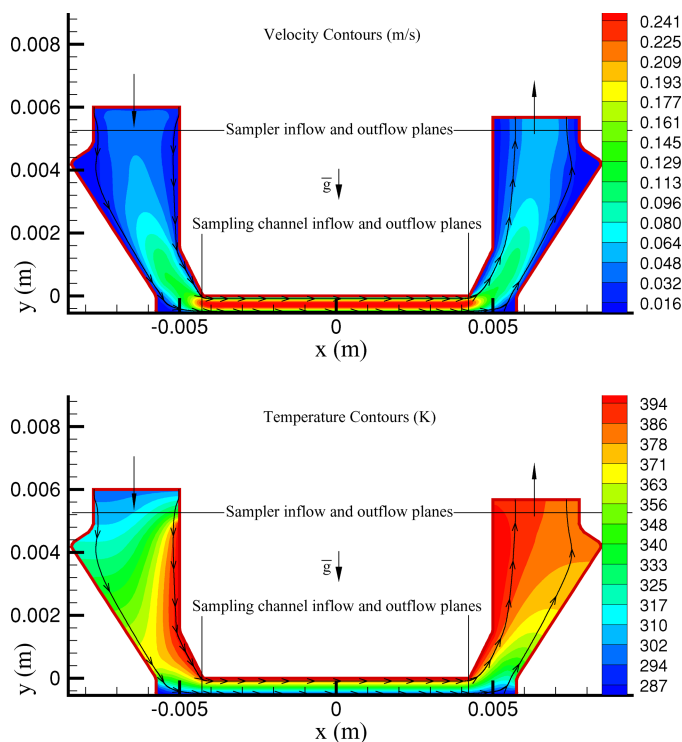


FIG. 2. (Color online) CFD calculations of flow and heat transfer in the TP at a flow rate of 27 sccm and a thermal gradient of 2200 K/cm.

105

110

115

120

125

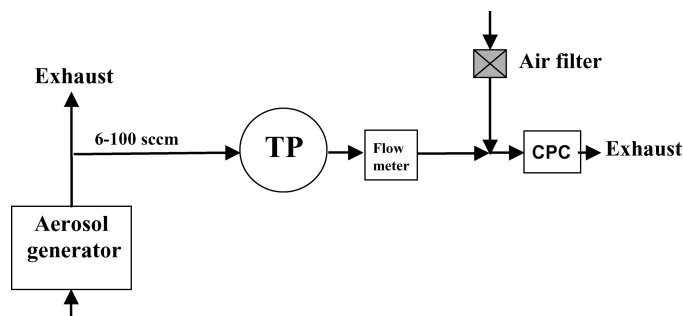


FIG. 3. Schematic of the experimental setup.

3. EXPERIMENTAL

3.1. Materials and Methods

The experimental setup used in this study is shown in Figure 3. It comprises an aerosol generator, a TP and particle size and concentration measurement equipment. In the experiments, two kinds of aerosol generators, a Collision-type nebulizer and a hot wire generator (HWG), were used. A filtered deionized water solution of NaCl (0.1 wt.%) was nebulized by the Collision-type atomizer operated with air (10 l/min). The number size distribution of NaCl particles was measured by a differential mobility analyzer system consisting of a charger, a classifier (modified Hauke, analyzer length 11 cm, sheath air and excess flow 23 l/min) and a condensation particle counter (CPC, TSI 3027).

Iron particles were synthesized using the HWG under a gaseous mixture of H_2/N_2 (mole component ratio 7/93) at 0.9 l/min. The HWG is a resistively heated thin iron wire (0.25 mm in diameter) located inside a glass bulb (Nasibulin et al. 2005). Number size distribution of iron particles was measured by a high resolution differential mobility analyzer (HR-DMA), (Gamero-Castaño and Fernandez de la Mora 2000; Nasibulin et al. 2002). Particles were charged by employing a radioactive ionizing source (^{241}Am) upstream of the classifier. The HR-DMA has a resolution of 2.1–2.5% in electrical mobility of a single charged particle of 1 nm which enables us to accurately measure the aerosol distribution including particle sizes below 3 nm. This resolution was determined from the peak width of pure electrospray (Fenn et al. 1989) tetraheptylammonium ions ($(C_7H_{15})_4N^+$) (Rosell-Llompart et al. 1996). DMA voltages “V” were converted to mobilities “Z” based on the linear relation between V and 1/Z (at fixed flow rates) and using, as a standard, the mobility of $(C_7H_{15})_4N^+$ with the reference value of $0.962 \text{ cm}^2/V/s$ reported by Gamero-Castaño and Fernandez de la Mora (2000).

Subsequently, the absolute size of Fe particles was determined from the mobility by using the modified empirical formula given by Shandakov et al. (2005). The sheath flow rate inside the classifier was maintained at 315 l/min. The sheath air flow was filtered upstream of the DMA by means of a HEPA filter. The concentration of classified particles was measured by an electrometer. An electrostatic precipitator was used to col-

lect the aerosol particles on a carbon coated copper grid. The morphology and the primary particle size of generated particles were investigated by means of a field emission scanning electron microscope (Leo Gemini DSM982) and a field emission transmission electron microscope (Philips CM200 FEG).

Aerosol particles passed through the TP at different flow rates which were accurately controlled using an absolute bubble flow meter. Aerosol flow rates were varied from 10 sccm to 100 sccm. The thermophoretic deposition efficiency was assessed experimentally from the aerosol concentration measured on-line using a condensation particle counter where the deposition efficiency, η_{eff} , is defined as

$$\eta_{eff} = \frac{(C_o - C_i)}{C_o} \times 100\% \quad [1]$$

where C_i and C_o are the particle concentrations measured after TP when a thermal gradient was applied and when it was zero, respectively. This definition of deposition efficiency effectively removes the contribution of other transport mechanisms (such as Brownian diffusion) which are not strongly affected by the temperature gradient in the gas.

In order to estimate the number size distribution of particles deposited along the TP, NaCl particles were collected on thin aluminium foil substrates. A fixed thermal gradient of 2200 K/cm was used in all the experiments. Statistical measurements of the particle size distribution were carried out on the basis of scanning electron micrographs taken at three different areas of the substrate. These areas were close to the inlet, in the middle and close to the outlet of the TP (Area 1, Area 2 and Area 3, respectively). Experiments were carried out at aerosol flow rates of 30 sccm and 60 sccm through TP with a collection time of 15 minutes. The size of about 300 particles was measured for each sample.

Homogeneity of the deposition was estimated on the basis of the density of NaCl particles deposited on the aforementioned areas of the substrate while varying the aerosol flow rate from 6 sccm to 60 sccm. Additionally, the uniformity of the deposition of Fe nanoparticles along the TP was also tested through a visual study of TEM images of samples collected on 3 mm carbon-coated copper microscope grids using a flow rate of 60 sccm.

3.2. Theoretical Aspects

The theoretical deposition efficiency, η_{eff} , in the TP was calculated using Eq. 1. The spatial distribution of aerosol particles at the entrance of the TP is assumed to be uniform. It is also assumed that the aerosol deposition due to diffusion in the TP when a thermal gradient was applied is the same as in the case of zero gradient, as was confirmed by two dimensional calculations.

The thermophoretic deposition efficiency in accordance with Eq. 1 at the conditions of the applied thermal gradient was

calculated as

$$\eta_{\text{eff}}/100\% = y_L/h, \quad [2]$$

where y_L is the height position coordinate starting from the cold plate in the TP channel, determined according to the condition:

$$L = \int_0^{y_L} \frac{u}{V_T} dy. \quad [3]$$

The last equation is derived for a uniform particle distribution at the inlet of the TP with the assumption that the thermophoretic transport to the cold walls before and after the deposition chamber is negligible and the walls outside the deposition chamber are adiabatic. Consequently, heat transfer and thermophoretic deposition on these walls are neglected.

It is obvious that the motion of the particles along the coordinate y is largely determined by the thermophoretic velocity V_T , while the motion in the TP along the flow direction (x coordinate) is largely determined by the rate of the gas flow u .

The velocity of the thermophoresis was calculated according to the expression for small particles, namely at Knudsen's number larger than 3:

$$V_T = -\frac{3}{8} \frac{\mu \nabla T}{0.499 \rho T (1 + \pi \alpha / 8)} = -\kappa \nu \frac{\nabla T}{T}. \quad [4]$$

Here, μ and ν are a dynamic and kinematic gas viscosity; ρ is a gas density; $\nabla T = dT/dy$ is the temperature gradient between plates; α is an accommodation coefficient; $k = 0.54$ is a numerical coefficient estimated at $\alpha = 1$ (Fuchs 1964).

The temperature between plates with temperatures of T_0 at $y = h$ and T_1 at $y = 0$ was calculated assuming one-dimensional heat transfer

$$\lambda dT/dy = J_T = \text{const} \quad [5]$$

in accordance with the approach of narrow channel and slow motion (Lapin et al. 1989). Here, λ is a gas thermal conductivity and J_T is a heat flux module.

The integration of Eq. 5 taking into account boundary conditions gives the following solution:

$$y = \frac{f_1(T) - f_1(T_1)}{J_T}, \quad J_T = \frac{f_1(T_0) - f_1(T_1)}{h}, \quad [6]$$

where we introduced a function, $f_1(T)$, defined as

$$f_1(T) = \int \lambda(T) dT. \quad [7]$$

In this case the temperature gradient may be calculated as

$$\frac{dT}{dy} = \frac{f_1(T_0) - f_1(T_1)}{\lambda h}, \quad [8]$$

The gas velocity between the plates in the TP was calculated in accordance with Stocks equation in the approximation of narrow channel and slow motion (Lapin et al. 1989):

$$\frac{\partial}{\partial y} \mu \frac{\partial u}{\partial y} = C, \quad [9]$$

with the following boundary conditions:

$$u(0) = u(h) = 0 \text{ or } u(T_1) = u(T_0) = 0. \quad [10]$$

The constant, C , in Eq. 9 is defined according to the conservation of mass. The velocity is expressed as:

$$\begin{aligned} \bar{u} &= \frac{Q}{ah} = \frac{1}{h} \int_0^h \frac{\rho}{\rho_{\text{entr}}} u dy = \frac{1}{h} \int_0^h \frac{T_{\text{entr}}}{T} u dy \\ &= \int_{T_1}^{T_0} \frac{T_{\text{entr}}}{T} \frac{\lambda}{f_1(T_0) - f_1(T_1)} u dT, \end{aligned} \quad [11]$$

where Q is a volumetric flow rate; ρ_{entr} is a gas density at room temperature, T_{entr} (temperature at the TP entrance). The ratios, $\rho/\rho_{\text{entr}} = T_{\text{entr}}/T$, in Eq. 11 were calculated in accordance with the state equation of ideal gases in the approach of constant pressure at slow gas motion.

Taking into account Eqs. 10–11, the solution of Eq. 9 can be written as

$$u = \bar{u} \frac{f_1(T_0) - f_1(T_1)}{T_{\text{entr}}} \frac{J(T) - I(T)}{J_{\text{int}} - I_{\text{int}}}, \quad [12]$$

where functions $I(T)$, $J(T)$, J_{int} and I_{int} are introduced and defined as

$$\begin{aligned} I(T) &= \int_{T_1}^T \frac{\lambda}{\mu} dT \Big/ \int_{T_1}^{T_0} \frac{\lambda}{\mu} dT, \quad J(T) \\ &= \int_{T_1}^T \frac{\lambda}{\mu} f_1(T) dT \Big/ \int_{T_1}^{T_0} \frac{\lambda}{\mu} f_1(T) dT, \\ J_{\text{int}} &= \int_{T_1}^{T_0} \frac{\lambda}{T} J(T) dT, \quad I_{\text{int}} = \int_{T_1}^{T_0} \frac{\lambda}{T} I(T) dT. \end{aligned}$$

In order to define the gas velocity profile in the TP the temperature dependence of the gas thermal conductivity coefficient, λ , and viscosity must be determined. In the present work the temperature dependence of the gas thermal conductivity coefficient, λ , was determined on the basis of the N -th order polynomial form (Reid et al. 1977):

$$\lambda = \sum_{i=0}^N a_i T^i. \quad [13]$$

Thermal conductivity coefficient of $\text{N}_2\text{-H}_2$ mixture is calculated by using Ulybkin's empirical relation (Reid et al. 1977)

on the basis of its experimental value at normal temperature of $T = 273.16 \text{ K}$ ($\lambda = 0.02736 \text{ W} \cdot \text{m}^{-1} \text{K}^{-1}$) (Hirschfelder et al. 1954). In this case coefficients in Eq. (13) are taken as $a_0 = -5.56087 \cdot 10^{-4} \text{ W} \cdot \text{m}^{-1} \text{K}^{-1}$, $a_1 = 1.14343 \cdot 10^{-4} \text{ W} \cdot \text{m}^{-1} \text{K}^{-2}$ and $a_2 = -4.44585 \cdot 10^{-8} \text{ W} \cdot \text{m}^{-1} \text{K}^{-3}$ (Babichev et al. 1991). The temperature dependence of viscosity was determined according to (Reid et al. 1977):

$$\mu = \mu_0(T/T_0)^b, \quad [14]$$

where b is a constant determined on the basis of experimental data (0.7708 and 0.6907 for air and H_2/N_2 , respectively). Viscosity of the mixture is calculated using Wilke's method (Reid et al. 1977). Taking into account Eqs. 13–14, the integrals (Eq. (12)) can be written as

$$I(T) = \frac{f_{1-b}(T) - f_{1-b}(T_1)}{f_{1-b}(T_0) - f_{1-b}(T_1)}, \quad J(T) = \frac{B_1^{1-b}(T) - B_1^{1-b}(T_1)}{B_1^{1-b}(T_0) - B_1^{1-b}(T_1)}, \quad [15]$$

$$I_{\text{int}} = \frac{B_{1-b}^0(T_0) - B_{1-b}^0(T_1)}{f_{1-b}(T_0) - f_{1-b}(T_1)} - \frac{f_0(T_0) - f_0(T_1)}{f_{1-b}(T_0) - f_{1-b}(T_1)} f_{1-b}(T_1), \quad [16]$$

$$J_{\text{int}} = \frac{\sum_{i=0}^N \frac{a_i}{i+1} (B_{2-b+i}^0(T_0) - B_{2-b+i}^0(T_1))}{B_1^{1-b}(T_0) - B_1^{1-b}(T_1)} - \frac{f_0(T_0) - f_0(T_1)}{B_1^{1-b}(T_0) - B_1^{1-b}(T_1)} B_1^{1-b}(T_1), \quad [17]$$

where we introduced a functions, $f_n(T)$ and $B_k^n(T)$, defined as

$$f_0(T) = a_0 \ln T + \sum_{i=1}^N \frac{a_i}{i} T^i, \quad f_n(T) = \sum_{i=0}^N \frac{a_i}{n+i} T^{n+i} (n > 0),$$

$$B_k^n(T) = \sum_{i=0}^N \frac{a_i}{k+i} f_{k+n+i}(T). \quad [18]$$

Temperature dependence of the viscosity was determined on the basis of the experimental data reported by Babichev et al. (1991). The molecule diameters were determined according to the Lennard-Jones potentials (Reid et al. 1977). The gas temperature at the TP entrance was taken to be $T_{\text{entr}} = 298 \text{ K}$. The algorithm of the calculations of the TP efficiency was the following. First, according to Eq. 6 we found the temperature distribution between the TP plates. Second, according to Eqs. 12, 15–17, the appropriate gas velocity distribution in the TP was calculated. Further, one can calculate the thermophoretic rate according to expression (4). The coordinate of the particle, y_L , at the entrance to and at the outlet from the TP was found on the basis of the Eq. 3. If the particle beginning its motion from the hot plate, passed the distance less than the cold plate, L , then the TP efficiency was taken as 100%. Otherwise the

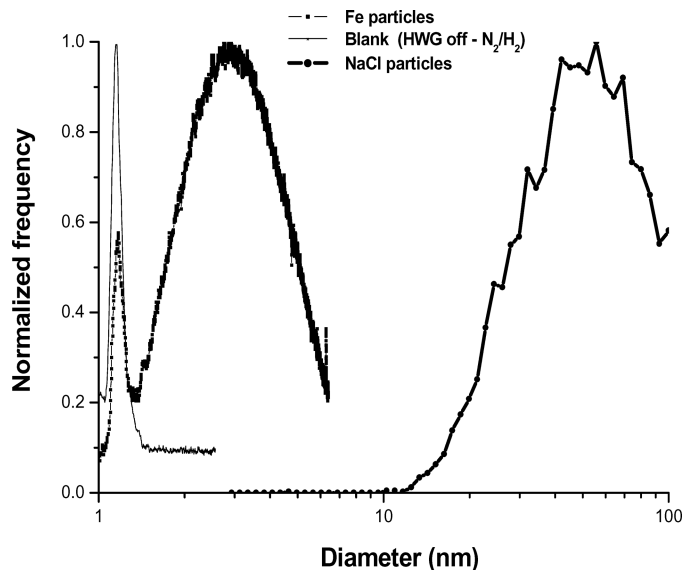


FIG. 4. Electrical mobility distributions (normalized to 1) of Fe and NaCl particles used for the testing of the TP.

efficiency was calculated according to Eq. 1 taking into account Eq. 2

4. RESULTS AND DISCUSSION

4.1. Particle Characterization

Normalized electrical mobility distributions of generated particles are illustrated in Figure 4. Total particle number concentration was about 10^6 particles/cm³ for both Fe and NaCl particles. In these experiments, Fe particles clearly present lower mobility diameters and narrower size distribution to that of NaCl particles. Mean diameters of 3.6 nm and 46.3 nm and geometric standard deviations of 1.40 and 1.57 were calculated for Fe and NaCl particles, respectively. It is worth noting that, in the case of the distribution measured by HR-DMA, an additional peak at diameters below 1.3 nm has been observed. However, this peak was attributed to the ions generated by the radioactive source according to the mobility spectra obtained with the HWG turned off Figure 4.

4.2 Thermophoretic Deposition Efficiency

Both experimental and theoretical data (in accordance with the described algorithm) of the deposition efficiency of NaCl and Fe particles at average thermal gradients of 2200 K/cm (1900 K/cm at the hot plate and 2500 K/cm at the cold one) and 2400 K/cm (2000 K/cm at the hot plate and 2800 K/cm at the cold one) are plotted versus the aerosol flow rate in Figures 5a–b, respectively.

Results show that high deposition efficiencies are attained at low flow rates. Thus, maximum efficiency values approaching 100%, i.e. the TP working as a gas filter, are achieved when aerosol flow rate was 10 sccm. Furthermore,

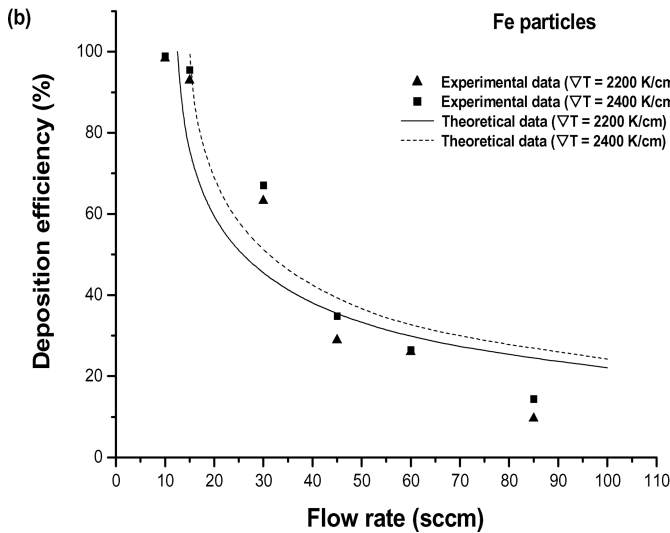
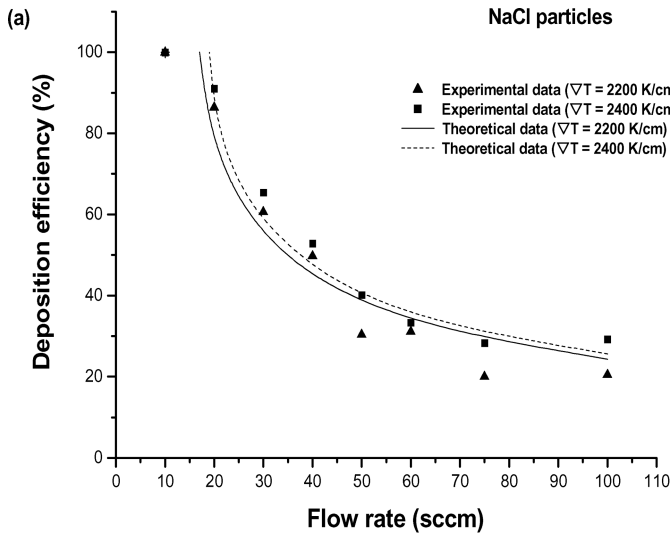


FIG. 5. Thermal deposition efficiency of (a) NaCl and (b) Fe particles as a function of the flow rate: experimental data and numerical calculations.

the thermophoretic deposition efficiency gradually decreases as the flow rate increases, which is in agreement with the theoretical calculations. As an example, as the flow rate varies from 10 sccm to 100 sccm, a decay in the deposition efficiency from ~100% to ~20% is observed for the collection of NaCl particles when the thermal gradient is 2200 K/cm.

Figures 5a–b also reveal a similar tendency in the efficiency, regardless the type of aerosol for the whole range of flows studied. Moreover, an increase in the thermal gradient applied between the hot and cold elements inside the TP leads to similar efficiency values for both aerosol samples. Thus, the percentage difference of the deposition efficiency remains below 10% when the thermal gradient is varied from 2200 K/cm to 2400 K/cm in the whole range of flow rates studied for both NaCl and Fe particles.

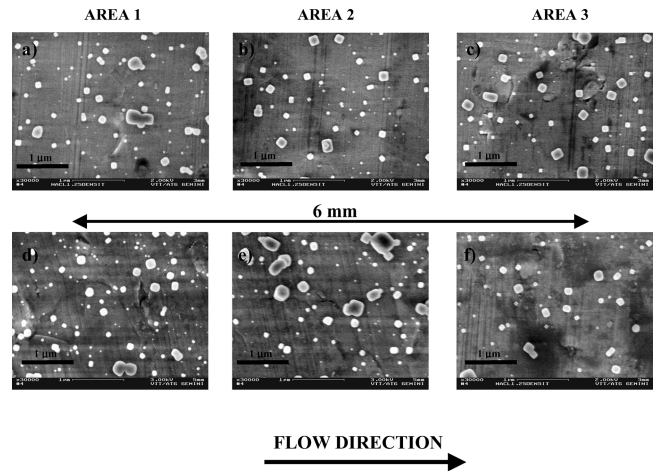


FIG. 6. SEM images of NaCl particles deposited on the substrate along the flow direction (Areas 1-3) at 50 sccm (a–c) and 12 sccm (d–f). Distance between the zones of the substrate Area 1 and Area 3 was 6 mm. Particle collection time was 15 min.

A comparison between experimental and theoretical data shows that experimental thermophoretic deposition efficiencies agree very well with the theoretical predictions.

4.3 Uniformity of the Aerosol Deposition

NaCl particles were deposited on thin foil substrates using a fixed thermal gradient of 2200 K/cm. Different regions of the substrate (Area 1, Area 2 and Area 3) along the flow direction were selected to estimate the particle deposition density.

A simple visual study of SEM micrographs of the NaCl particles deposited on the substrates using an aerosol flow rate of 50 sccm (Figures 6a–c) fairly shows a high degree of homogeneity of the aerosol deposition inside the TP. Moreover, the deposited

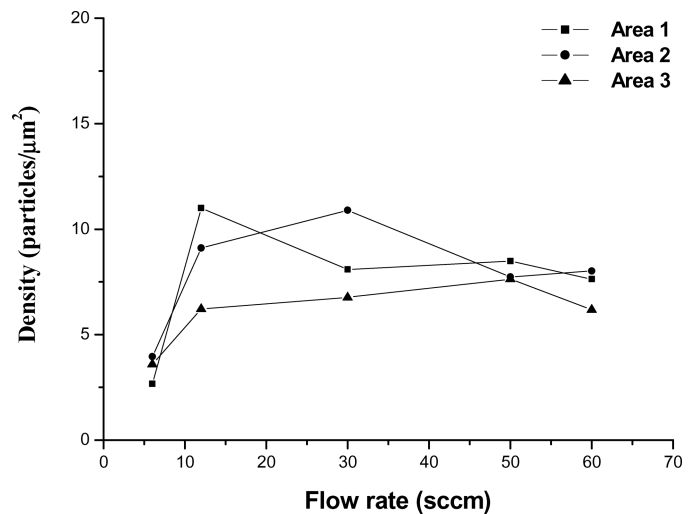


FIG. 7. Particle density of NaCl particles estimated from SEM images at the selected zones of the substrate (Areas 1–3) as a function of the aerosol flow rate. Particle collection time was 15 min.

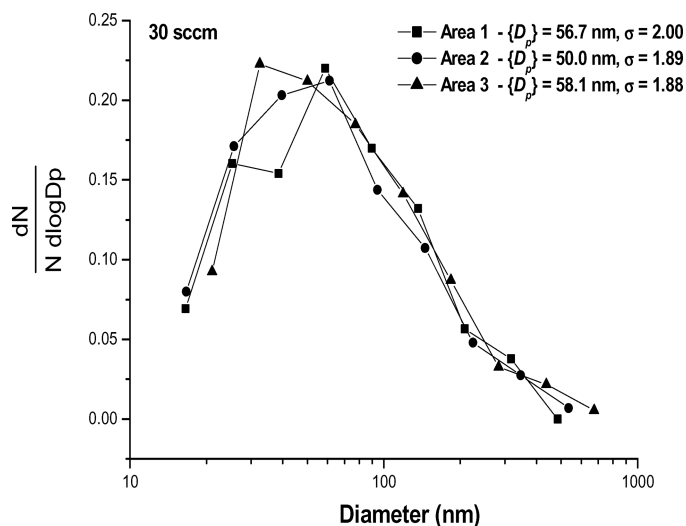


FIG. 8. Normalized number size distribution of NaCl particles measured from SEM images taken at different zones of the substrate (Areas 1–3) using aerosol flow rates of 30 sccm.

NaCl particle concentration using aerosol flow rates between 6 sccm and 60 sccm is shown in Figure 7. As can be seen, aerosol deposition of NaCl particles occurs uniformly along the TP precipitation zone, especially at the highest and lowest flow rates. It is also worth noting that this tendency was found to be slightly different when flow rates of 12 sccm and 30 sccm were used. In these cases the thermophoretic deposition seems to take place preferentially near the inflow or the intermediate zone of the TP sampling channel. However, the uniformity of deposition might still be considered satisfactory under these conditions as can be seen from SEM images of NaCl particles collected using a flow rate of 12 sccm.

Figure 8 shows particle size distributions of NaCl particles deposited on Areas 1–3 at a flow rate of 30 sccm which were estimated on the basis of SEM images. Similar mean values of

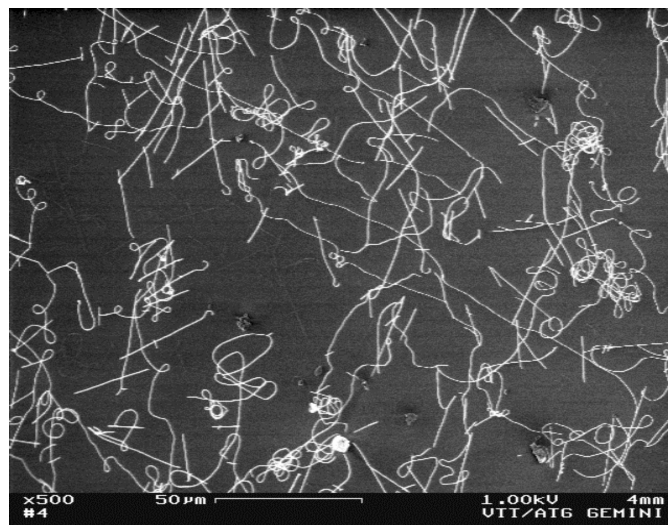


FIG. 10. SEM image of carbon nanotubes synthesised by chemical vapour deposition method using thermophoretically collected Fe particles onto SiO₂ substrates.

~57 nm, 50 nm and 58 nm were obtained from the size distribution of aerosol particles collected on areas 1, 2 and 3, respectively. These results indicate that the deposition of NaCl particles along the TP was homogeneous and largely independent of the particle size.

Uniform deposition of Fe nanoparticles onto substrates was also observed. As can be seen from Figure 9, when Fe particles were collected on two microscope support grids separated by 6 mm at a flow rate of 60 sccm, a homogenous deposition was accomplished.

4.4. Utilization of Thermophoretically Deposited Iron Particles as Catalyst for Growing CNTs

Iron catalyst particles were produced by vaporization/condensation with the HWG and thermophoretically deposited

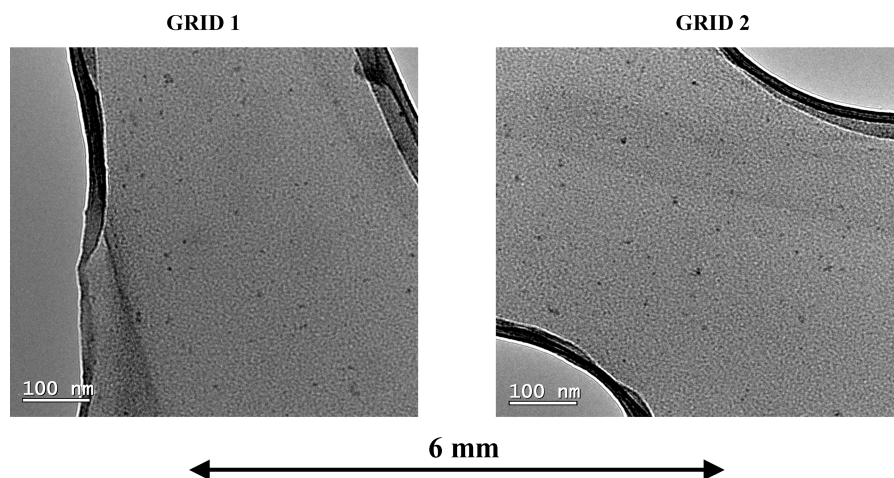


FIG. 9. TEM images of Fe particles collected for 15 min by TP at a flow rate of 60 sccm. Images were taken at two zones of the support grids (Grid 1–2) separated by a distance of 6 mm within thermal precipitator.

380 on SiO₂ substrates using the described TP. Iron particles were
 carried into the TP using an H₂/N₂ gas mixture (mole component
 ratio 93/7) with a flow rate of 60 sccm. The collection time was
 1 hour. The synthesis of the CNTs was carried out by a chemical
 vapour deposition method using a vertical flow laminar reactor.
 385 CO was used as the carbon source. Inside the reactor, CO dispropo-
 ntionation took place on the surface of metal particles leading
 to the formation of CNTs. SEM images of SiO₂ substrates shown
 in Figure 10 clearly reveal the successful synthesis of CNTs from
 the deposited Fe particles.

390 5. CONCLUSIONS

An efficient thermophoretic precipitator has been designed,
 constructed and used for collection of nanometer-sized aerosol
 particles. The device allows efficient collection of particles di-
 rectly onto various substrates, for instance, transmission electron
 microscope support grids, SiO₂ substrates, *etc.* The precipitator
 395 was tested using NaCl and Fe particles with geometric number
 mean diameters of 50 nm and 3.6 nm, respectively. The study
 of the thermophoretic efficiency clearly showed that the depo-
 sition approaches 100% when the aerosol flow rate was below
 400 15 sccm. Furthermore, the deposition efficiency experimental
 data for Fe and NaCl nanoparticles was found to agree fairly
 well with computational simulation. According to the particle
 density determined on different areas of the substrates, high uni-
 formity in the NaCl and Fe deposition at the millimeter scales
 405 were attained. Particle collection was shown to be homogeneous
 in the TP regardless the particle size. Finally, carbon nanotubes
 (CNTs) were successfully grown on SiO₂ substrates using TP
 collected Fe catalyst particles.

REFERENCES

- 410 Bang, J. J., Trillo, E. A., and Murr, L. E. (2003). Utilization of selected area
 electron diffraction patterns for characterization of air submicron particu-
 late matter collected by a thermophoretic precipitator, *J. Air Waste Manage.*
 53:227–236.
- 415 Babichev, A. P., Babushkina, N. A., Bratkovskii, A. M. et al. (1991). Fizicheskie
 velichiny: Spravochnik (Physical quantities: A handbook). Energoatomizdat,
 Moscow.
- Brock, J. R. (1962). On the theory of thermal forces acting on aerosol particles,
J. Colloid Sci. 17:768–770.
- 420 Brown, D. P., Biswas, P., and Rubin, S. G. (1994). Transport and Deposition of
 Particles in Gas Turbines: Effects of Convection, Diffusion, Thermophoresis,
 Inertial Impaction and Coagulation. Proceedings of the 1994 international
 joint power generation. The Fuels and combustion technologies (FACT) divi-
 sion, ASME. Phoenix, Arizona, p. 69.
- 425 Brown, D. P., Kauppinen, E. I., Jokiniemi, J. K., Biswas, P., and Rubin, S. G.
 (2005). A Method of Moments Based CFD Model for Polydisperse Aerosol
 Flows with Strong Interphase Mass and Heat Transfer, *Submitted to Comput-
 ers and Fluids.*
- Fenn, J. B., Mann, M., Meng, C. K., Wong, S. K., and Whitehouse, C. (1989).
 Electrospray ionization for mass spectrometry of large biomolecules, *Science*
 246:64–71.
- Fu, L., Cao, L., Liu, Y., and Zhu, D. (2004). Molecular and nanoscale materials 430
 and devices in electronics, *Adv. Colloid. Interfac.* 111:133–157.
- Fuchs, N.A. (1964). The Mechanics of Aerosols. Pergamon Press, Oxford.
- Gamero-Castaño, M., and Fernández de la Mora, J., (2000). Mechanisms of
 electrospray ionization of singly and multiply charged salt clusters, *Anal.* 435
Chim. Acta 406:67–91.
- Green, H. L., and Watson, H. H. (1935). Physical methods for the estimation of
 the dust hazard in industry, *Med. Res. Council Spec. Rept.* HMS, London.
- Hirschfelder, J. O., Curtis, F., and Bird, R. B. (1954). Molecular Theory of gases
 and liquids. John Wiley and Sons, New York.
- Kethley, T. W., Gordon, M. R., and Orr, C. (1952). A thermal precipitator for 440
 aerobacteriology, *Science* 116:368–369.
- Kodas, T., and Hampden-Smith, M. (1999). Aerosol processing of materials.
 Wiley, New York.
- Lapin, Yu. V., and Strelets, M. Kh. (1989). Internal gas mixtures flows. Nauka,
 Moscow. 445
- Maynard, A. D. (1995). The development of a new thermophoretic precipitator
 for scanning transmission electron microscope analysis of ultrafine aerosol
 particles, *Aerosol Sci. Tech.* 23:521–533.
- Montassier, N., Boulaud, D., and Renoux, A. (1991). Experimental study of ther-
 mophoretic particle deposition in laminar tube flow, *J. Aerosol Sci.* 22:677– 450
 687.
- Nasibulin, A. G., Kauppinen, E. I., Thomson, B. A., and Fernandez de la Mora,
 J. (2002). TEM imaging of mass-selected polymer molecules, *Journal of*
Nanoparticle Research 4:449–453.
- Nasibulin, A. G., Moisala, A., Jiang, H., and Kauppinen, E. I. (2005). Carbon 455
 nanotube synthesis from alcohols by a novel aerosol method. Accepted, *to*
Journal of Nanoparticle Research.
- Pitkethly, M. (2003). Nanoparticles as building blocks?, *Materialstoday.* 6:36–
 42.
- Pui, Y. H. D., and Chen, D. (1997). Nanometer particles: A new frontier for 460
 multidisciplinary research, *J. Aerosol Sci.* 28:539–544.
- Reid, R. C., Prausnitz J. M., and Sherwood, T. K. (1977). The properties of gases
 and liquids. McGraw-Hill, New York.
- Romay, F. J., Takagaki, S. S., Pui, D. Y. H., and Liu, B. Y. H. (1998). Ther-
 mophoretic deposition of aerosol particles in turbulent pipe flow, *J. Aerosol* 465
Sci. 29:943–959.
- Rosell-Llompart, J., Loscertales, I. G., Bingham, D., and Fernandez de la Mora,
 J. (1996). Sizing nanoparticles and ions with a short differential mobility
 analyzer, *J. Aerosol Sci.* 27:695–719.
- Shandakov, S. D., Nasibulin, A. G., and Kauppinen, E. I. (2005). Phenomenolog- 470
 ical description of mobility of nm- and sub-nm-sized charged aerosol particles
 in electric field, *J. Aerosol Sci.* In press, doi:10.1016/j.jaerosci.2005.01.003.
- Stratmann, F., Otto, E., and Fissan, H. (1994). Thermophoretic and diffusional
 particle transport in cooled laminar tube flow, *J. Aerosol Sci.* 25:1305–
 1319. 475
- Tsai, C.-J., and Lu, H.-C. (1995). Design and evaluation of a plate-to-plate ther-
 mophoretic precipitator, *Aerosol Sci. Tech.* 22:172–180.
- Tsai, C.-J., Lin, J.-S., Aggarwal, S. G., and Chen, D.-R. (2004). Thermophoretic
 deposition of particles in laminar and turbulent flows, *Aerosol Sci. Tech.* 480
 38:131–139.
- Wright, B. M. (1953). Gravimetric thermal precipitator, *Science* 118:195.
- Zheng, F. (2002). Thermophoresis of spherical and non-spherical particles: A
 review of theories and experiments, *Adv. Colloid. Interfac.* 97:255–278.